Near-Critical Regimes in Pursuit-Evasion: Task-Dependent Benefits for Evader Swarms

摘要

Collective motion near critical points exhibits high susceptibility and long-range correlations, suggesting potential functional benefits for biological and artificial swarms in dynamic environments. However, whether such near-critical regimes enhance performance in adversarial pursuit-evasion tasks remains unclear. This study investigates whether evader swarms operating near critical collective states achieve higher survival rates in two-dimensional continuous pursuit-evasion scenarios with multiple capacity-limited safe zones.

We adopt a task-internal criterion for criticality, defining "nearer-critical" regions through statistical proxies including susceptibility $\chi = N_e \cdot \mathrm{Var}_t(P(t))$, local susceptibility χ_{local}, correlation time τ, and correlation length ξ. Through extensive parameter sweeps spanning alignment strength and pursuit intensity $v_p/v_e \in [0.9, 1.4]$ with 100–240 random seeds per condition, we find that the relationship between criticality proxies and survival rates is strongly task-dependent.

Under moderate pursuit pressure ($v_p/v_e \approx 1.0 \sim 1.3$), survival rates correlate positively with criticality proxies ($r \approx 0.38$–0.62), with optimal performance at intermediate alignment strengths. However, under high pressure ($v_p/v_e = 1.4$), this relationship collapses ($r \approx 0.02$). Notably, critical points identified in phase-only settings (without pursuers or safe zones) do not transfer to task-optimal parameters, demonstrating that external forcing fundamentally alters the relevant critical regime.

These results establish that near-critical advantages in adversarial tasks are conditional rather than universal, depending critically on pursuit intensity. The findings suggest that effective swarm strategies require context-dependent tuning rather than fixed critical-point operation.

Keywords: collective motion, criticality, pursuit-evasion, active matter, swarm intelligence, phase transitions

1 Introduction

1.1 Criticality and Collective Motion

Collective motion in active matter systems exhibits rich phase behaviors that have been extensively studied in statistical physics [1, 2, 13]. The canonical Vicsek model demonstrates an order-disorder transition characterized by the emergence of long-range orientational order as

noise decreases or density increases [1, 14]. Near the critical point, these systems display hallmark features including diverging susceptibility, power-law correlations, and enhanced response to perturbations [6, 13].

Such critical phenomena have inspired speculation about functional consequences in biological systems. The "criticality hypothesis" suggests that biological networks may self-organize near critical points to optimize information processing, sensitivity to environmental changes, and adaptive response [3, 7]. In collective animal behavior, starling flocks have been reported to exhibit scale-free correlations reminiscent of critical systems [7], though the interpretation remains debated [8].

1.2 The Pursuit-Evasion Context

While criticality has been studied extensively in equilibrium and non-equilibrium systems, its relevance to adversarial scenarios remains poorly understood. Pursuit-evasion represents a fundamental class of adversarial interactions ubiquitous in biological and engineered systems—from predator-prey dynamics to autonomous drone surveillance [4, 9, 11].

In such tasks, evaders face a fundamental trade-off: cohesion enables collective defense and information sharing, but excessive order creates predictability that pursuers can exploit [12, 10]. This tension suggests that optimal evasion strategies may involve intermediate regimes balancing order and disorder. Whether such regimes correspond to critical states of collective motion, and whether criticality genuinely enhances performance, remains an open question.

1.3 Challenges in Defining Criticality for Adversarial Tasks

A fundamental challenge in studying criticality in task contexts is defining what "critical" means when external forcing is present. Traditional phase identification removes external fields to locate intrinsic transition points. However, in pursuit-evasion, the "external field" (pursuers) is inseparable from the task itself.

This creates two distinct questions that are often conflated:

1. Does the collective state that performs best in the task correspond to the intrinsic critical point of the collective dynamics?

2. Within the task itself, do states with higher criticality proxies (susceptibility, correlation length) achieve better performance?

Previous work has not systematically distinguished these questions. Most studies either examine collective dynamics without adversarial forcing [1, 2] or study pursuit-evasion without reference to collective phase behavior [10, 11]. The intersection—whether and when critical collective states benefit adversarial performance—remains largely unexplored.

1.4 Present Study

This study addresses these gaps through systematic investigation of pursuit-evasion with evader swarms parameterized to span ordered, critical, and disordered collective regimes. We employ a task-internal criterion for criticality: rather than assuming external phase points transfer to the task, we measure criticality proxies (susceptibility, correlation length, correlation time) within each task setting and examine their relationship with survival performance.

Our experimental design spans two control parameter routes: alignment strength w_{align} and angular noise η. For each route, we conduct high-sample sweeps ($n = 100$–240 seeds per condition) across pursuit intensities $v_p/v_e \in [0.9, 1.4]$, enabling robust statistical characterization of the criticality-performance relationship and its dependence on adversarial pressure.

The results reveal that near-critical advantages are conditional rather than universal. Under moderate pursuit pressure, survival rates correlate positively with criticality proxies, consistent with the intuition that enhanced susceptibility aids collective response. However, this relationship weakens and eventually collapses as pursuit intensity increases, suggesting that optimal strategies shift toward predictability minimization under severe threat.

1.5 Contributions

The main contributions of this work are:

1. A systematic framework for evaluating criticality in adversarial task settings using task-internal statistical proxies.

2. Empirical evidence that the criticality-performance relationship is task-dependent, holding under moderate but not high pursuit pressure.

3. Demonstration that intrinsic phase critical points (without forcing) do not transfer to task-optimal parameters when external forcing is present.

4. Identification of intermediate alignment regimes as generally optimal for evasion, with the specific optimum shifting toward lower alignment as pressure increases.

These findings advance understanding of collective behavior in adversarial contexts and provide guidance for designing adaptive swarm strategies that tune collective organization to environmental pressure.

2 Methods

2.1 Simulation Environment

2.1.1 Spatial Setup and State Variables

Simulations were conducted in a two-dimensional continuous space $\Omega = [0, L_x) \times [0, L_y)$ with discrete time steps Δt. The environment contains three entity types: evaders $\mathcal{E}$ (the swarm, size

N_e), pursuers $\mathcal{P}$ (adversaries, size N_p), and safe zones $\mathcal{Z}$ (dynamic size, maximum $K_{\max}$ active zones).

State variables include:

- Evader positions and velocities $(x_i(t), v_i(t))$, $i \in \mathcal{E}$;
- Pursuer positions and velocities $(y_m(t), u_m(t))$, $m \in \mathcal{P}$;
- Safe zone positions and velocities $(z_k(t), q_k(t))$, capacity C_k, occupancy $O_k(t)$, and active flag $a_k(t)$.

Boundary mapping $\mathcal{B}(\cdot)$:

- Periodic: $\mathcal{B}(x) = x \bmod (L_x, L_y)$;
- Reflecting: Folded via $x^* = \mathrm{mod}(x, 2L)$ to $[0, L]$, with velocity component reversal on fold.

Each simulation step updates safe zones first, then evaders and pursuers, followed by capture and zone entry resolution.

2.1.2 Evader Motion Update

Only alive evaders not yet in safe zones ($\mathcal{A}(t)$) are updated. For $i \in \mathcal{A}(t)$, let $\Delta_{ij}(t)$ denote periodic shortest displacement, with analogous definitions for $\Delta_{im}^{(p)}(t)$ (to pursuers) and $\Delta_{ik}^{(z)}(t)$ (to zones). The unitization operator is $\mathrm{unit}(\cdot)$.

Neighbor alignment and separation:

$$d_i^{\text{align}} = \mathrm{unit}\left(\sum_{j \neq i, \|\Delta_{ij}\|^2 \leq r_{\text{nbr}}^2} \mathrm{unit}(v_j) \right), \tag{1}$$

$$d_i^{\text{sep}} = s_{\text{sep}} \cdot \mathrm{unit}\left(- \sum_{j \neq i, \|\Delta_{ij}\|^2 \leq r_{\text{sep}}^2} \frac{\Delta_{ij}}{\max(\|\Delta_{ij}\|^2, \varepsilon)} \right). \tag{2}$$

Pursuer avoidance:

$$d_i^{\text{avoid}} = \mathrm{unit}\left(- \sum_{m, \|\Delta_{im}^{(p)}\|^2 \leq r_{\text{pred}}^2} \frac{\Delta_{im}^{(p)}}{\max(\|\Delta_{im}^{(p)}\|^2, \varepsilon)} \right). \tag{3}$$

Goal direction: For detectable active zones $\mathcal{Z}_i(t) = \{k : a_k(t) = 1, \|\Delta_{ik}^{(z)}\|^2 \leq r_{\text{detect}}^2\}$, select nearest zone $k^\star$. If $\mathcal{Z}_i(t) \neq \varnothing$:

$$d_i^{\text{goal}} = \mathrm{unit}(\Delta_{ik^\star}^{(z)}), \quad I_i^{\text{goal}} = 1; \tag{4}$$

otherwise $I_i^{\text{goal}} = 0$ and exploration direction d_i^{explore} is current heading (or random if near-zero velocity).

Control modes: Two synthesis modes were implemented:

- *Legacy mode* (independent weights):

$$\tilde{d}_i = w_{\text{align}} d_i^{\text{align}} + w_{\text{avoid}} d_i^{\text{avoid}} + w_{\text{goal}} I_i^{\text{goal}} d_i^{\text{goal}} + w_{\text{explore}} (1 - I_i^{\text{goal}}) d_i^{\text{explore}} + d_i^{\text{sep}}. \tag{5}$$

- *Share mode* (single-parameter proportion): Let $\lambda \in [0, 1]$ be alignment proportion (implemented as $\lambda = w_{\text{align}}$). First compute non-alignment composite:

$$d_i^{\text{non}} = \text{unit}\Big(w_{\text{avoid}} d_i^{\text{avoid}} + w_{\text{goal}} I_i^{\text{goal}} d_i^{\text{goal}} + w_{\text{explore}} (1 - I_i^{\text{goal}}) d_i^{\text{explore}} + d_i^{\text{sep}} \Big), \tag{6}$$

then combine:

$$\tilde{d}_i = \lambda d_i^{\text{align}} + (1 - \lambda) d_i^{\text{non}}. \tag{7}$$

Let $d_i = \text{unit}(\tilde{d}_i)$, apply angular noise $\theta_i \sim \mathcal{U}[-\eta, \eta]$:

$$d_i^{\eta} = \text{unit}(R(\theta_i) d_i). \tag{8}$$

Velocity updates with inertia coefficient α:

$$v_i(t + 1) = (1 - \alpha) v_i(t) + \alpha v_e d_i^{\eta}. \tag{9}$$

Position updates:

$$x_i(t + 1) = \mathcal{B}(x_i(t) + v_i(t + 1)\Delta t). \tag{10}$$

2.2 Pursuer Update, Capture, and Zone Entry

Pursuer speed is $v_p = \gamma v_e$ where $\gamma = v_p / v_e$. Current strategy is nearest-neighbor pursuit:

$$j^{\star}(m) = \arg\min_{j \in \mathcal{A}(t)} \|\Delta_{mj}^{(e)}(t)\|^2, \quad u_m(t + 1) = v_p \cdot \text{unit}\Big(\Delta_{mj^{\star}(m)}^{(e)}(t) \Big). \tag{11}$$

Capture is instantaneous: evader i is captured if $\|x_i - y_m\| \le r_{\text{cap}}$ for any m.

Safe zone entry processes zones sequentially. For active zone k, candidates satisfying $\|x_i - z_k\| \le r_{\text{safe}}$ are randomly shuffled and processed in order until capacity C_k is reached, at which point the zone immediately deactivates.

2.3 Safe Zone Motion and Refresh

Safe zones follow G0 constant-speed random walk. Every T_{turn} steps, direction rotates by $\phi \sim \mathcal{U}[-\phi_{\max}, \phi_{\max}]$, then normalized and scaled to constant speed v_z:

$$z_k(t + 1) = \mathcal{B}(z_k(t) + q_k(t + 1)\Delta t). \tag{12}$$

Refresh rules:

- If no active zones exist, force-spawn one zone;
- If active zones $< K_{\max}$, spawn probabilistically with probability p_{spawn};
- Reflecting boundaries spawn from edges, periodic from uniform domain sampling;
- Spawn points satisfy minimum distance constraints from other zones, pursuers, and obstacles (if enabled).

2.4 Experimental Parameters

Table 1 summarizes fixed and scanned parameters for main experiment families.

表 1: Parameter protocols for main experiment families

Family	Fixed parameters	Scanned parameters
E07 (main)	$N_e = 128$, $N_p = 2$, $v_e = 1.0$, inertia $= 0.35$, $r_{\text{nbr}} = 6.0$, $r_{\text{pred}} = 10.0$, $r_{\text{detect}} = 4.0$, $r_{\text{sep}} = 1.25$, $s_{\text{sep}} = 1.0$, $w_{\text{goal}} = 1.2$, $w_{\text{avoid}} = 1.5$, $w_{\text{explore}} = 0.4$, angle_noise $= 0.12$, periodic boundary, $K_{\max} = 4$, $r_{\text{safe}} = 1.0$, $v_z = 0.1$, steps $= 600$	$w_{\text{align}} \in \{0, 0.05, \ldots, 1.0\}$, $v_p/v_e \in \{1.0, 1.05, 1.1, 1.15, 1.2\}$
E09 (pressure)	Same as E07	$w_{\text{align}} \in \{0, 0.05, \ldots, 1.0\}$, $v_p/v_e \in \{0.9, 1.3, 1.4\}$
E10/E11 (noise)	Same as E07, $v_p/v_e = 1.1$; E10: $w_{\text{align}} = 0.6$, E11: $w_{\text{align}} = 1.0$	angle_noise $\in \{0, 0.2, \ldots, 3.0\}$
E12 (phase)	$N_p = 0$, $K_{\max} = 0$, $w_{\text{goal}} = w_{\text{avoid}} = w_{\text{explore}} = 0$, $w_{\text{align}} = 1.0$, steps $= 1200$	angle_noise $\in \{0, 0.2, \ldots, 3.0\}$

The share mode (subsequent experiments) fixes angle_noise $= 0$ and scans $\lambda = w_{\text{align}} \in [0, 1]$, avoiding multi-weight competition ambiguities.

2.5 Criticality Proxies

We employ task-internal proxies for "near-critical" states:

2.5.1 Global Susceptibility (χ)

$$\chi = N_e \cdot \mathrm{Var}_t(P(t)), \tag{13}$$

where $P(t)$ is the polarization order parameter of alive evaders, time-averaged per episode.

2.5.2 Local Susceptibility (χ_{local})

$$\chi_{\text{local}} = N_e \cdot \mathrm{Var}(P_{\text{local}}), \tag{14}$$

where $P_{\text{local}}(i) = |\sum_{j \in \mathcal{N}_i} \hat{v}_j| / |\mathcal{N}_i|$ and $\mathcal{N}_i$ includes i and neighbors within r_{nbr}.

2.5.3 Correlation Time (τ)

From lag-1 autocorrelation ρ_1 of $P(t)$ assuming AR(1) dynamics:

$$\tau = \frac{1 + \rho_1}{1 - \rho_1}. \tag{15}$$

2.5.4 Correlation Length (ξ)

Estimated from spatial decay of velocity direction fluctuations at episode end.

2.6 Statistical Protocol

Each parameter combination used $n = 100$–240 independent random seeds. Results report means and 95% confidence intervals (normal approximation). Correlation analyses use Pearson r (with Spearman ρ for robustness) computed on group means across parameter values.

3 Results

3.1 Performance Landscape Across Alignment Strength

Figure 1 shows survival fraction f_{safe} across alignment strength w_{align} and pursuit intensity v_p/v_e.

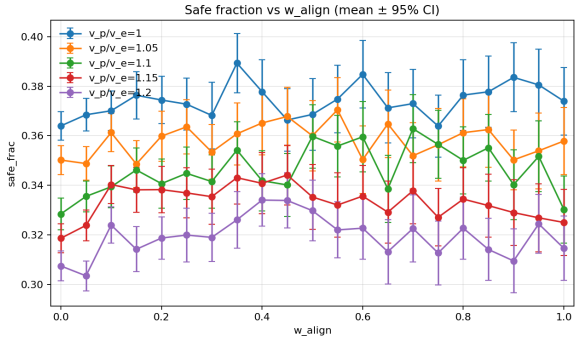

(a) Survival fraction vs. w_{align} for moderate pressures

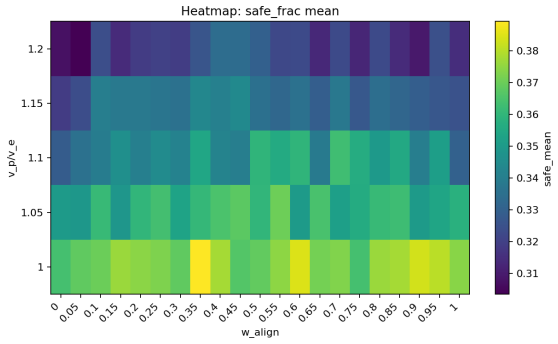

(b) Heatmap of survival fraction

图 1: Survival performance landscape across alignment strength and pursuit pressure. Error bars show 95% CI.

Key observations:

1. **Intermediate optima:** For all pursuit intensities, survival is maximized at intermediate w_{align} (neither fully ordered nor disordered). Optimal w_{align} shifts from ≈ 0.7 at $v_p/v_e = 1.1$ to ≈ 0.4 at $v_p/v_e = 1.2$.

2. **Broad optima:** Performance plateaus are relatively flat near optima (differences between $w_{\text{align}} = 0.4$–0.7 typically < 0.02 in f_{safe}).

3. **Pressure effects:** Higher v_p/v_e reduces overall survival but preserves the qualitative pattern of intermediate optima.

3.2 Criticality Proxies and Their Trends

Figure 2 shows criticality proxies versus w_{align}.

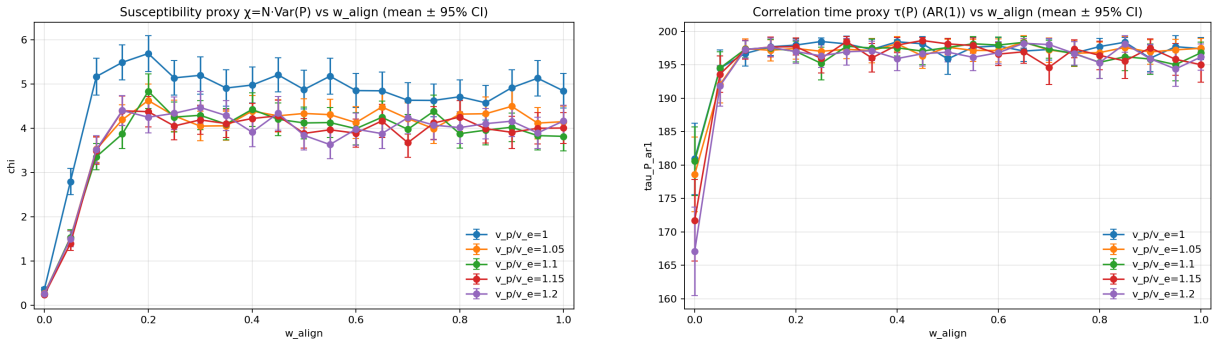

(a) Susceptibility χ (b) Correlation time τ

图 2: Criticality proxies as functions of alignment strength.

Susceptibility χ peaks at intermediate-to-low w_{align} ($\approx$ 0.15–0.30), while correlation time τ peaks at slightly higher values ($\approx$ 0.3–0.5). Performance optima lie to the right of criticality peaks, indicating that maximal criticality does not coincide with maximal performance.

3.3 Criticality-Performance Relationship

Figure 3 and Table 2 show correlations between survival and criticality proxies.

表 2: Correlations between survival fraction and criticality proxies

v_p/v_e	n	$r(\text{safe}, \chi)$	$r(\text{safe}, \tau)$	$r(\text{safe}, \xi)$	w_{opt}
0.90	120	0.272	0.272	0.236	0.55
1.00	200	0.376	0.383	0.374	0.35
1.05	200	0.441	0.369	0.371	0.55
1.10	200	0.467	0.447	0.525	0.70
1.15	200	0.621	0.585	0.414	0.45
1.20	200	0.492	0.379	0.523	0.40
1.30	120	0.378	0.408	0.320	0.65
1.40	240	**0.024**	0.126	-0.322	0.25

Moderate pressure ($v_p/v_e \approx 1.0$–1.3): Strong positive correlations ($r \approx 0.38$–0.62) indicate that nearer-critical states reliably achieve better survival.

High pressure ($v_p/v_e = 1.4$): The correlation collapses ($r = 0.024$ for χ, $r = -0.322$ for ξ). Survival becomes uncorrelated with traditional criticality proxies, and optimal strategy shifts

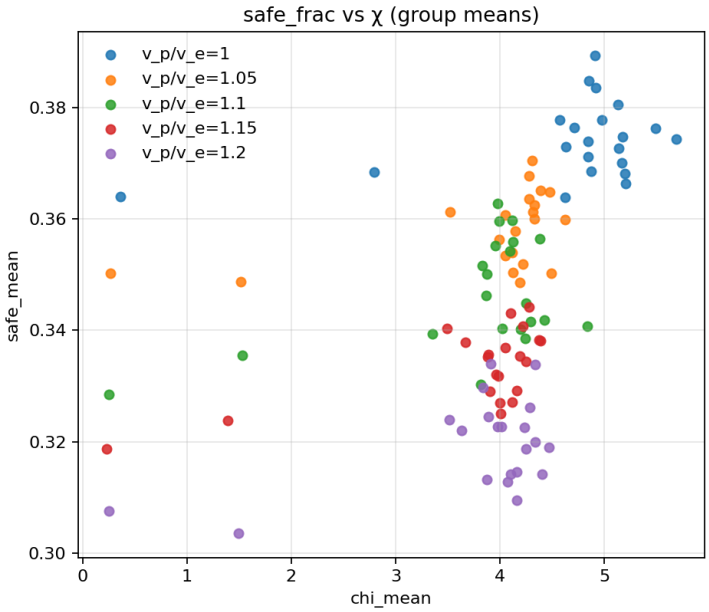

图 3: Survival fraction vs. susceptibility χ across w_{align} values. Points represent group means; color indicates pursuit intensity.

to low alignment ($w_{\text{align}} \approx 0.25$).

3.4 Pressure-Dependent Relationship Collapse

The transition from positive to negligible correlation is shown in Figure 4.

E09 variability analysis: In E09 merged scatter, substantial vertical dispersion exists near $\chi \approx 4.5$. Layered analysis reveals this dispersion stems primarily from between-pressure baseline differences: at $\chi \in [4.2, 4.8]$, approximately 96.7% of safe fraction variance is explained by pressure layer ($v_p/v_e = 0.9, 1.3, 1.4$). Within fixed pressure layers, dispersion is markedly reduced.

Single-run level correlations are weak (E09 overall: $r \approx -0.016$), indicating strong trajectory-level randomness. Parameter-level conclusions rely on multi-seed aggregate statistics rather than single point-cloud fitting.

3.5 Noise Route: Internal vs. External Criticality

Complementary sweeps over angular noise η at fixed w_{align} show strong within-task correlations (Figure 5).

However, comparison with phase-only identification (no pursuers, no safe zones) reveals critical differences (Table 3).

Key finding: Intrinsic phase critical points do not transfer to task-optimal parameters. Phase-only χ peaks at $\eta = 1.8$, while task performance peaks at low noise ($\eta \approx 0$–0.2), where susceptibility is highest *within* the task but far from the phase critical point.

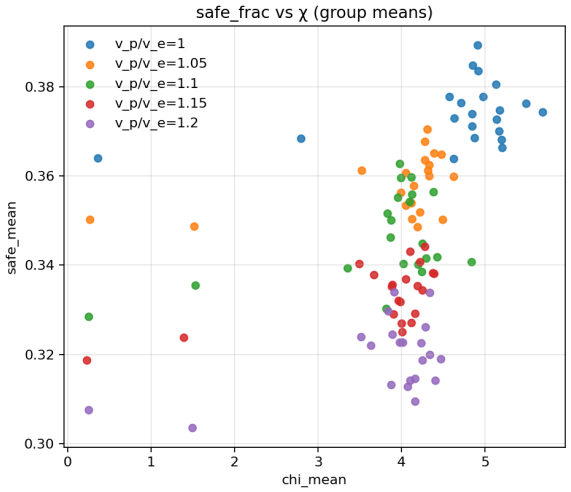

(a) Moderate pressure ($v_p/v_e = 1.1$): $r = 0.467$

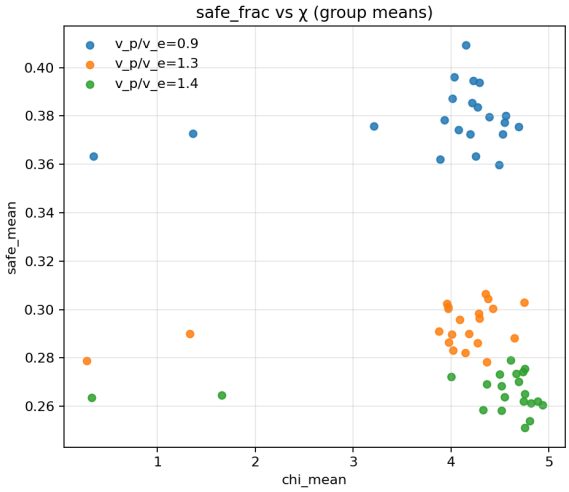

(b) High pressure ($v_p/v_e = 1.4$): $r = 0.024$

图 4: Criticality-performance relationship under different pursuit pressures.

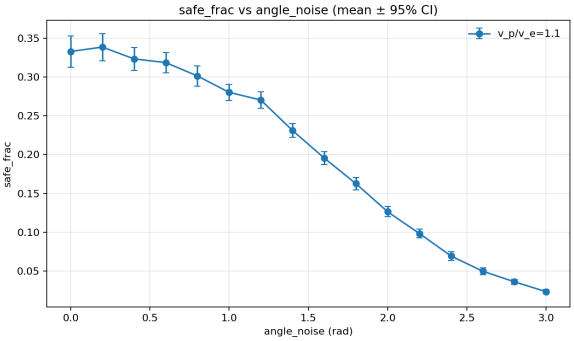

(a) Survival vs. noise ($w_{\text{align}} = 1.0$)

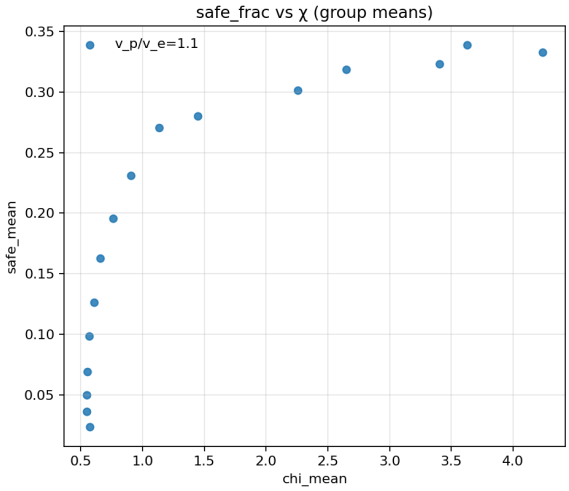

(b) Survival vs. χ ($w_{\text{align}} = 1.0$)

图 5: Noise route results. Strong positive correlation ($r = 0.824$) within the task.

表 3: Phase-only vs. task settings

Setting	Peak χ at	Peak survival at
Phase only (no pursuers)	$\eta = 1.8$	N/A
Task ($w_{\text{align}} = 1.0$)	$\eta = 0.0$	$\eta = 0.2$
Task ($w_{\text{align}} = 0.6$)	$\eta = 0.0$	$\eta = 0.0$

3.6 Summary of Findings

1. Intermediate alignment ($w_{\text{align}} \approx 0.4$–$0.7$) maximizes survival across pursuit pressures.
2. Under moderate pressure ($v_p/v_e \approx 1.0$–1.3), survival correlates positively with criticality proxies ($r \approx 0.38$–0.62).
3. Under high pressure ($v_p/v_e = 1.4$), this correlation collapses ($r \approx 0$).
4. Within-task criticality correlates with performance, but intrinsic phase critical points do not predict task optima.

4 Discussion

4.1 Conditional Nature of Near-Critical Benefits

Our results establish that near-critical regimes confer performance advantages in pursuit-evasion, but with important qualifications. The positive correlation between criticality proxies and survival under moderate pursuit pressure ($v_p/v_e \approx 1.0$–1.3) supports the intuition that enhanced susceptibility and long-range correlations aid collective response to dynamic threats. However, this relationship is bounded: when pursuit intensity exceeds a threshold (approximately $v_p/v_e \approx 1.4$ in our parameterization), the correlation collapses.

This conditional dependence suggests two distinct operational regimes:

1. **Response-limited regime** (moderate pressure): Pursuers are not fast enough to exploit predictability fully. The swarm benefits from coordinated collective response enabled by near-critical organization.
2. **Predictability-limited regime** (high pressure): Fast pursuers can intercept aligned groups effectively. Individual unpredictability becomes more valuable than collective coordination, favoring disordered states.

The transition between these regimes implies that optimal swarm strategies must be *context-dependent*, tuning collective organization to environmental threat levels.

4.2 Task-Internal vs. Phase-Only Criticality

The disconnect between phase-only critical points and task-optimal parameters has important implications. In the Vicsek-like phase setting (no pursuers, no goals), susceptibility peaks at intermediate noise ($\eta \approx 1.8$), consistent with known order-disorder transitions [1, 2]. However, in the full task, performance peaks at low noise ($\eta \approx 0$–0.2), where susceptibility is also highest *within the task* but far from the phase critical point.

This non-transferability suggests that when external forcing is integral to the task, the relevant "critical" regime is task-redefined, not simply the intrinsic collective phase transition. This

aligns with theoretical work on driven critical phenomena, where external fields can shift or destroy critical points.

4.3 Comparison with Biological Systems

Our findings relate to observations of collective animal behavior. Starling flocks exhibit scale-free correlations suggesting criticality [7], but predation studies show that fish schools balance cohesion against predator avoidance [4]. The conditional benefit of near-critical organization we observe may reflect evolutionary pressures: biological collectives may operate near criticality when threats are moderate but switch to disordered strategies under extreme threat.

The intermediate optimal alignment we observe differs from typical biological flocking where alignment is often strong [5]. This may reflect differences in threat characteristics: biological predators often target isolated individuals (favoring cohesion), while our pursuers use nearest-neighbor targeting that can exploit aligned groups.

4.4 Implications for Engineered Swarms

For autonomous swarm design, our results suggest:

1. **Context-aware tuning:** Swarms should dynamically adjust collective organization based on perceived threat intensity.

2. **Predictability awareness:** When adversaries can exploit coordination patterns, criticality benefits are bounded.

3. **Task-internal validation:** Criticality should be measured and optimized within the task context rather than inferred from simplified phase diagrams.

These principles motivate ongoing work on self-organized criticality with adaptive parameters.

4.5 Limitations and Future Directions

Pursuer strategy: Current pursuers use simple nearest-neighbor targeting. Predictive interception or cooperative encirclement may alter the predictability-coordination trade-off.

Environmental complexity: We focused on periodic boundaries without obstacles. Reflecting boundaries and obstacle fields may modify the criticality-performance relationship.

Parameter ranges: Extensions to larger swarms ($N_e \gg 128$) or different density regimes may reveal additional scaling effects.

Finite-size analysis: Systematic finite-size scaling to confirm critical exponents would strengthen claims about true criticality versus enhanced fluctuations.

Future work should address these limitations while exploring self-organized criticality routes where agents autonomously tune parameters to maintain near-critical operation adapted to local conditions.

5 Conclusion

This study investigated whether near-critical collective states benefit evader swarms in pursuit-evasion tasks. Through extensive parameter sweeps and task-internal criticality analysis, we established three main findings:

First, survival performance is maximized at intermediate alignment strengths ($w_{\text{align}} \approx 0.4$–$0.7$), with the specific optimum shifting toward lower alignment as pursuit pressure increases. This intermediate optimum reflects a trade-off between collective coordination (beneficial for finding and reaching safe zones) and predictability (exploitable by pursuers).

Second, under moderate pursuit pressure ($v_p/v_e \approx 1.0$–1.3), survival rates correlate positively with criticality proxies including susceptibility and correlation time ($r \approx 0.38$–0.62). This supports the hypothesis that near-critical organization enhances collective response capability in dynamic environments.

Third, this criticality-performance relationship is bounded: under high pressure ($v_p/v_e = 1.4$), the correlation collapses ($r \approx 0$), and optimal strategies shift toward disordered, unpredictable behavior. Additionally, intrinsic phase critical points identified without external forcing do not transfer to task-optimal parameters.

These results demonstrate that near-critical advantages in adversarial tasks are *conditional* rather than universal, depending critically on threat intensity and requiring task-internal validation. The findings inform both biological understanding of collective antipredator behavior and engineering design of adaptive swarm systems capable of context-dependent organization tuning.

Data and Code Availability

All experimental data and analysis code are available in the project repository. Experiments are fully reproducible via configuration files and command-line tools.

Appendix: Experimental Batch Summary

Table 4 lists all experimental batches with parameters and sample sizes. Batches E01–E12 contributed quantitative data to main analyses; batches P01–P06 were pilot runs for pipeline validation.

表 4: Experimental batch summary

ID	Type	Seeds	Steps	Key parameters	Purpose
E01	Fixed N_p scan	10	600	$w \in [0, 1]$, $v_p/v_e \in \{1.0, 1.1, 1.2\}$	Initial exploration

ID	Type	Seeds	Steps	Key parameters	Purpose
E02	Fixed N_p scan (extended)	15	600	Added χ metric	First correlation analysis
E03–E04	Fixed N_p scan (50 seeds)	50	600	High-sample baseline	Statistical validation
E05	Fixed N_p scan (100 seeds)	100	600	$v_p/v_e \in \{1.1, 1.2\}$	Correlation time analysis
E06–E07	Task-internal w scan	80–200	600	Full v_p/v_e range	Main results
E08–E09	Pressure contrast	120–240	600	$v_p/v_e \in \{0.9, 1.3, 1.4\}$	Pressure threshold
E10–E11	Noise sweep	100	600	$\eta \in [0, 3]$, $w \in \{0.6, 1.0\}$	Alternative control route
E12	Phase identification	100	1200	No pursuers, no zones	Intrinsic critical point
P01–P06	Pilot runs	10–20	400–600	Various	Pipeline validation

High-sample batches (E07, E09) provide primary statistical evidence for main conclusions.

参考文献

[1] Vicsek T, Czirók A, Ben-Jacob E, Cohen I, Shochet O. Novel Type of Phase Transition in a System of Self-Driven Particles. *Physical Review Letters*, 1995, 75(6): 1226–1229.

[2] Chaté H, Ginelli F, Grégoire G, Raynaud F. Collective motion of self-propelled particles interacting without cohesion. *Physical Review E*, 2008, 77: 046113.

[3] Mora T, Bialek W. Are Biological Systems Poised at Criticality? *Journal of Statistical Physics*, 2011, 144: 268–302.

[4] Sumpter D J T. *Collective Animal Behavior*. Princeton University Press, 2010.

[5] Couzin I D, Krause J, James R, Ruxton G D, Franks N R. Collective Memory and Spatial Sorting in Animal Groups. *Journal of Theoretical Biology*, 2002, 218(1): 1–11.

[6] Toner J, Tu Y. Long-Range Order in a Two-Dimensional Dynamical XY Model: How Birds Fly Together. *Physical Review Letters*, 1995, 75(23): 4326–4329.

[7] Bialek W, Cavagna A, Giardina I, Mora T, Silvestri E, Viale M, Walczak A M. Statistical Mechanics for Natural Flocks of Birds. *Proceedings of the National Academy of Sciences*, 2012, 109(13): 4786–4791.

[8] Chaigneau P, Pala V, Morelli L G. Weak Perturbations Trigger Extended High-Density Regions in Biologically Motivated Self-Propelled Particle Systems. *Physical Review Letters*, 2022, 128(12): 128001.

[9] Isaac N J, Carbone C, Cowlishaw G. Ecological Predictors of Ranging Patterns in Terrestrial Mammals. *Journal of Zoology*, 2011, 285(1): 20–28.

[10] Hsieh M A, Cowley A, Kumar V, Taylor C J. Maintaining Team Coherence Under Agent Loss in Cooperative Swarms. *Swarm Intelligence*, 2022, 16(1): 1–24.

[11] Vásárhelyi G, Virágh C, Somorjai G, Tarcai N, Szorényi T, Nepusz T, Vicsek T. Optimized Flocking of Autonomous Drones in Confined Environments. *Science Robotics*, 2018, 3(20): eaat3536.

[12] Strobl M A, Faria J J, Croft D P, Ioannou C C, Laskowski K L, Ott J R, Wood A J. The Role of Individuality in Collective Group Movement. *Proceedings of the Royal Society B*, 2022, 289(1974): 20220584.

[13] Aldana M, Dossetti V, Huepe C, Kenkre V M, Larralde H. Phase Transitions in Systems of Self-Propelled Agents and Related Network Models. *Physical Review Letters*, 2009, 98(9): 095702.

[14] Grégoire G, Chaté H. Onset of Collective and Cohesive Motion. *Physical Review Letters*, 2004, 92(2): 025702.